Theor Chem Acc (2012) 131:1088
DOI 10.1007/s00214-012-1088-z

REGULAR ARTICLE

Proton-bound homodimers involving second-row atoms

Bun Chan · Janet E. Del Bene · Leo Radom

Received: 4 March 2011 / Accepted: 14 June 2011 / Published online: 10 February 2012

Abstract High-level ab initio quantum chemical calculations (G4(MP2)//MP2/6-311+G(2df,p)) have been used to examine homodimers of second-row bases, and to compare the results with those obtained previously for the first-row analogs. The relationship between the binding energies of the dimers and the proton affinities (PAs) of the bases follows the same pattern as that for the first-row systems, with the binding energies initially increasing with increasing proton affinity but subsequently decreasing. This may be attributed to the opposing effects of increased PA on the hydrogen-bond donor and hydrogen-bond acceptor. The binding energies are generally smaller for the second-row dimers than for the corresponding first-row dimers. There is an increased tendency for asymmetrical hydrogen bonds in homodimers of the second-row compared with first-row dimers. This may be attributed to the lower electronegativities of second-row atoms relative to their first-row counterparts, and to the longer internuclear separation between the hydrogen-bonded second-row atoms.

Keywords Hydrogen bonding · Ab initio · Homodimers · Binding energies · Structures

Dedicated to Professor Eluvathingal Jemmis and published as part of the special collection of articles celebrating his 60th birthday.

B. Chan (✉) · L. Radom (✉)
School of Chemistry and ARC Centre of Excellence for Free Radical Chemistry and Biotechnology, University of Sydney, Sydney, NSW 2006, Australia
e-mail: chan_b@chem.usyd.edu.au

L. Radom
e-mail: radom@chem.usyd.edu.au

J. E. Del Bene (✉)
Department of Chemistry, Youngstown State University, Youngstown, OH 44555, USA
e-mail: jedelbene@ysu.edu

1 Introduction

Hydrogen bonding has long been recognized as an important type of intermolecular interaction. Despite an extensive history, the structures, binding energies, and other spectroscopic properties of hydrogen-bonded complexes continue to be subjects of current interest and investigation [1–6]. Such studies are desirable, since hydrogen bonding plays a key role in determining the structures and properties of many chemical and biological systems, and understanding what occurs in these systems therefore requires an understanding of the hydrogen bond.

For a series of closely related proton-bound dimers, it has been found that the binding energies (BEs) of complexes are inversely related to the difference between the proton affinities (PAs) of the proton-donor (D) and proton-acceptor (A) molecules, provided that only a single minimum exists across the proton-transfer coordinate [6–12]. This is generally the case for first-row complexes, for which the closer the proton affinities of D and A, the stronger the binding. Therefore, for first-row complexes, it is generally the proton-bound homodimer that has the greatest binding energy. Such is not necessarily the case for second-row proton-bound complexes for which double minima can exist across the proton-transfer coordinate. In such situations, the highest binding energy is found for the complex in which the weaker base is protonated and acts as a proton donor to the stronger base [13].

In the present study, we are interested in the second-row proton-bound homodimers in which the bases D and A are the same. For these, the hydrogen bond may be represented

as $[RX\cdots H\cdots XR]^+$, with X representing the basic site at which the proton is bound. Proton-bound homodimers are of special interest due to their unusual properties compared with those of ordinary hydrogen-bonded complexes. For example, some homodimers have binding energies greater than 100 kJ mol^{-1} [8, 14–17] compared with binding energies for neutral complexes with typical hydrogen bonds that are generally no more than several tens of kJ mol^{-1} [1–6, 18–20]. The hydrogen bonds in these species are sometimes symmetric, that is, the two X···H distances are equal, and sometimes asymmetric. In the symmetric or near-symmetric cases, proton-shared hydrogen bonds are often formed in which the X···X distances can be shorter than twice the van der Waals radius of X.

We have previously investigated both the energies [21] and the structures [22] of proton-bound homodimers in which the donor/acceptor atom X is a first-row electronegative element (N, O, F, or Ne). In these studies, we addressed the relationship between hydrogen-bond energies of proton-bound dimers and the proton affinities of the corresponding bases, and the factors that determine whether a proton-bound homodimer has a symmetric or asymmetric hydrogen bond. Both the binding energy and geometry of such dimers are influenced by opposing effects related to the partial breaking of the X–H bond of the donor and the partial formation of the H···X bond with the acceptor. These opposing effects can lead to non-monotonic trends in binding energies and geometries among a series of closely related proton-bound homodimers.

It is of interest to examine whether the features observed previously for proton-bound homodimers of the first-row also apply to the proton-bound dimers of the second-row. In the present study, we address this question by examining proton-bound homodimers involving corresponding second-row atoms (P, S, Cl, or Ar).

2 Computational details

Standard ab initio molecular orbital theory calculations [23, 24] were carried out with the Gaussian 03 [25] and Gaussian 09 [26] programs. Geometries were obtained at the MP2/6-311+G(2df,p) level of theory. Unless otherwise noted, single-point energies were obtained at the G4(MP2) level. Vibrational frequencies were computed to identify equilibrium and transition structures with zero and one imaginary frequency, respectively. Vibrationless proton affinities (PA) of bases and binding energies (BE) of dimers were obtained as the negative of the energies for the respective reactions:

$$RX + H^+ \rightarrow RX\text{-}H^+ \quad (1)$$

$$RX\text{-}H^+ + RX \rightarrow [RX\cdots H\cdots XR]^+. \quad (2)$$

Unless otherwise noted, geometrical parameters in the text refer to MP2/6-311+G(2df,p) values, while relative energies are G4(MP2)//MP2/6-311+G(2df,p) vibrationless values. Natural bond orbital (NBO) population analysis was carried out at the MP2/6-311+G(2df,p) level. All reported bond lengths are in Å and relative energies are in kJ mol^{-1}.

One question that was addressed in our previous study and will be asked again is what factors determine whether a proton-bound homodimer has a symmetric or an asymmetric hydrogen bond. To assist in the analysis, we defined measures of the energy requirements to move from an asymmetrical to a symmetrical proton-bound dimer, and vice versa. In the case of a proton-bound dimer for which the equilibrium structure is asymmetrical, the symmetrization energy (ΔE_{sym}) can be defined as

$$\Delta E_{sym} = E_{sym} - E_{asym} \quad (3)$$

where E_{sym} is the energy of the constrained symmetric structure, while E_{asym} is the energy of the asymmetric equilibrium structure. For a dimer with a symmetrical equilibrium structure, it follows that $\Delta E_{sym} = 0$. In addition, it is convenient to define the distortion energy $[\Delta E_{dist}(\Delta r)]$ as

$$\Delta E_{dist}(\Delta r) = E_{dist}(\Delta r) - E_{sym} \quad (4)$$

where $E_{dist}(\Delta r)$ is the energy of a non-symmetrical structure in which all structural parameters are optimized except for the bonds to the shared proton, which are constrained to differ in length by Δr.

3 Results and discussion

The results of this study are subdivided into four sections as follows:

1. examination of relationships between binding energies and proton affinities for second-row bases and comparison with first-row bases;
2. analysis of proton affinities for first-row and second-row bases and comparison of the binding energies of their proton-bound dimers;
3. analysis of the structures of second-row versus first-row proton-bound homodimers; and
4. examination of the symmetrization energies and distortion energies for second-row proton-bound dimers.

3.1 Comparison of relationships between binding energies and proton affinities of first-row and second-row proton-bound homodimers

Figure 1 shows the BE–PA relationships for the prototypical first-row and second-row hydrides. The corresponding relationships between BEs and PAs for the second-row

bases in which H atoms are substituted in the parent molecules (H_3P, H_2S, HCl) by groups of varying electron-withdrawing or electron-donating ability are shown in Fig. 2. From Figs. 1 and 2 (and Fig. 3 in Ref. [21]), it is apparent that the correlations for first-row and second-row bases are similar. Thus, initially as the PA increases, the BE of the dimer also increases. However, at some point the BE starts to decrease as the PA increases. In our previous study of first-row bases, we attributed this to the opposing effects of increasing the PA of the hydrogen-bond-donor and hydrogen-bond-acceptor molecules [21]. Hydrogen-bond formation is associated with partial breaking of the X–H bond in the donor, and this becomes more difficult as the PA of X increases. On the other hand, formation of the new H···X bond becomes increasingly favorable as the PA of X increases. It is the compromise between these two effects that leads to the non-monotonic behavior in the BE–PA correlation. This is observed for both the first-row and second-row bases.

Within each subset (P, S, Cl), the BE and PA are related quadratically according to the following equations:

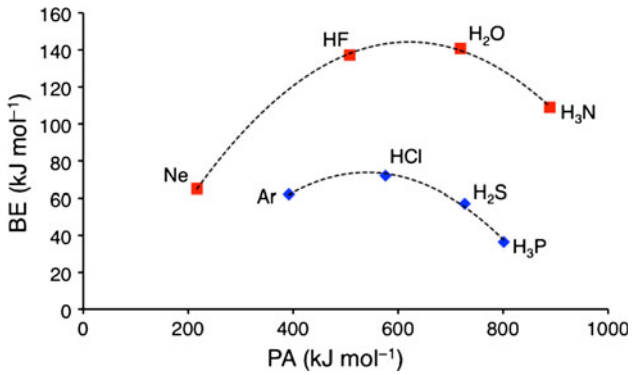

Fig. 1 Binding energies (BE, kJ mol^{-1}) of first-row and second-row proton-bound dimers versus proton affinities (PA, kJ mol^{-1}) of the corresponding bases

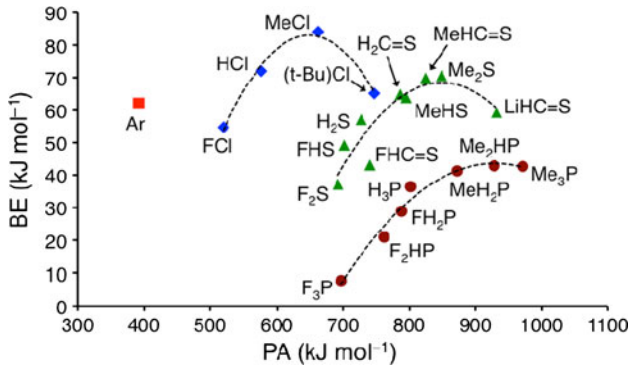

Fig. 2 Binding energies (BE, kJ mol^{-1}) of second-row proton-bound dimers versus proton affinities (PA, kJ mol^{-1}) of the corresponding bases

$$\text{P}: \ \text{BE} = -6.85 \times 10^{-4}\,\text{PA}^2 + 1.27\ \text{PA} - 547 \quad (5)$$

$$\text{S}: \ \text{BE} = -1.16 \times 10^{-3}\,\text{PA}^2 + 1.97\ \text{PA} - 766 \quad (6)$$

$$\text{Cl}: \ \text{BE} = -1.79 \times 10^{-3}\,\text{PA}^2 + 2.31\ \text{PA} - 666. \quad (7)$$

The corresponding equations that were found previously [21] for the first-row bases are:

$$\text{N}: \ \text{BE} = -5.69 \times 10^{-4}\,\text{PA}^2 + 0.981\ \text{PA} - 317 \quad (8)$$

$$\text{O}: \ \text{BE} = -7.61 \times 10^{-4}\,\text{PA}^2 + 1.14\ \text{PA} - 287 \quad (9)$$

$$\text{F}: \ \text{BE} = -1.57 \times 10^{-3}\,\text{PA}^2 + 1.74\ \text{PA} - 344. \quad (10)$$

An examination of the coefficients of PA^2 and PA in Eqs. 5–10 shows that for both first-row and second-row bases, the coefficients decrease in the order group 17 > group 16 > group 15. Thus, BEs for group 17 (halogen-group) proton-bound dimers are most sensitive to changes in the PA of the bases, while those for group 15 (nitrogen-group) dimers are least sensitive to PA changes.

3.2 Analysis of proton affinities for first-row and second-row bases and comparison of the binding energies of their proton-bound dimers

A closer examination of Fig. 1 reveals an interesting difference between first-row and second-row PAs. Although H_2S, HCl, and Ar have higher PAs than H_2O, HF, and Ne, respectively, the PA for H_3P is lower than that for H_3N. This is consistent with observations made in a previous study [27], which showed that the PAs for the nitrogen-group (group 15) hydrides decrease down the group, whereas the PAs increase for oxygen- (group 16), fluorine- (group 17), and neon- (group 18) group bases. Table 1 shows that there is a monotonic trend in the differences in proton affinities between first-row and second-row bases (ΔPA_{2-1}), which become more positive from group 15 (N/P) to group 18 (Ne/Ar). However, the fact that the second-row bases do not uniformly have higher or lower PAs than their first-row counterparts suggests that there are at least two opposing effects at work.

Table 1 provides data for two major factors that influence protonation at lone pairs: (1) the amount of electron density at X as measured by the NBO charge (Q) and (2) the polarizability (α) of X, which provides a measure of how easily the density can be transferred to the incoming proton. The data of Table 1 indicate that in going from a first-row to a second-row base, the polarizability increases significantly, and $\Delta\alpha_{2-1}$ is positive. This favors a greater PA for second-row bases. On the other hand, a second-row element is less electronegative than the corresponding first-row element. As a result, the central atom in a second-row base has a reduced electron density compared with the

Table 1 Proton affinities and dimer binding energies (kJ mol^{-1}) for bases H_nX, NBO atomic charges of X in H_nX, and the polarizability of atomic X

	First-row	Second-row	Δ_{2-1}
Proton affinity (H_nX)[a]			
H_3N/H_3P	888.9	801.3	−87.7
H_2O/H_2S	718.7	727.0	8.3
HF/HCl	507.8	576.0	68.2
Ne/Ar	216.9	391.9	175.0
Binding energy ($[H_nX–H\cdots XH_n]^+$)[a]			
H_3N/H_3P	108.9	36.5	−72.5
H_2O/H_2S	140.8	57.1	−83.6
HF/HCl	137.2	72.0	−65.2
Ne/Ar	65.1	62.1	−3.0
NBO charge (X in H_nX)[b]			
H_3N/H_3P	−1.030	0.163	1.193
H_2O/H_2S	−0.922	−0.224	0.699
HF/HCl	−0.560	−0.251	0.310
Ne/Ar	0.000	0.000	0.000
Polarizability (X)[c]			
N/P	7.26	24.93	17.67
S/O	5.24	19.37	14.13
F/Cl	3.70	14.57	10.87
Ne/Ar	2.68	11.10	8.42

[a] Obtained at the G3(MP2)-RAD//MP2/6-31+G(d,p) level for first-row bases [21] and the G4(MP2)//MP2-6-311+G(2df,p) level for second-row bases

[b] Calculated at the MP2/6-311+G(2df,p)//MP2/6-311+G(2df,p) level

[c] CCSD(T) values from Ref. [28]

corresponding first-row base, as reflected in the positive values of ΔQ_{2-1} in Table 1. This effect can be expected to be more pronounced as the number of X–H bonds in the base increases. Thus, for first-row bases the negative charge on X increases in the order HF < H_2O < H_3N. The second-row bases HCl and H_2S have small negative charges on Cl and S, Ne and Ar have no charge, and P has a positive charge, due to its slightly smaller electronegativity of 2.19 compared with that for H (2.20). The greater negative charge on X favors a higher PA for first-row bases. Since the second-row bases Ar, HCl, and H_2S have higher PAs than the corresponding first-row bases, it is the polarizability that dominates in these cases. However, a lack of a negative charge on P leads to a lower PA for H_3P than for H_3N.

It is also apparent from Table 1 and Fig. 1 that for group 15, 16, and 17 bases, the second-row proton-bound dimers have significantly smaller BEs than the corresponding first-row dimers. A closer examination of the changes in the BEs in going from first-row to second-row dimers (ΔBE_{2-1}) reveals a non-monotonic trend: H_3N/H_3P < H_2O/H_2S > HF/HCl ≫ Ne/Ar. How can this be explained? We have previously demonstrated that the charge on the donor atom is an important factor influencing the magnitude of the BE of a hydrogen-bonded complex [29]. However, as in the case of PAs, the increased polarizabilities of second-row bases can be expected to favor stronger hydrogen bonds. These two opposing effects also account for the non-monotonic trend in ΔBE_{2-1}. In contrast to the PAs, it is the charge on X that tends to dominate and make the BE of dimers of first-row hydrides significantly greater than dimers of second-row hydrides. However, as ΔQ_{2-1} decreases from group 15 to group 18, the polarizability assumes increased importance and leads to comparable BEs for $[Ar\cdots H\cdots Ar]^+$ and $[Ne\cdots H\cdots Ne]^+$.

3.3 Structures of second-row versus first-row proton-bound dimers

In our studies of first-row proton-bound homodimers, we observed that whether a proton-bound dimer has a symmetric or asymmetric X···H···X hydrogen bond is determined primarily by the electronegativity of X. Thus, dimers with F and O bases generally form complexes with symmetric hydrogen bonds (with the exception of one case involving an sp^2-hybridized oxygen base that also forms an intramolecular hydrogen bond). When the electronegativity is lowered by moving to N, then only *sp*-hybridized N bases tend to form symmetric hydrogen bonds, while sp^2 and sp^3 N bases form asymmetric hydrogen bonds. How do these findings for first-row homodimers compare with those for the second-row analogs?

The noble gases Ne and Ar form symmetric proton-bound dimers Ar_2H^+ and Ne_2H^+. Likewise, the proton-bound Cl dimers $(FCl)_2H^+$, $(HCl)_2H^+$, and $(MeCl)_2H^+$ have symmetric hydrogen bonds, as do the corresponding first-row dimers $(FF)_2H^+$, $(HF)_2H^+$, and $(MeF)_2H^+$.

The *sp*-hybridized base C≡S does not protonate at S nor does it form a stable proton-bound dimer at S. This behavior is quite different from its first-row analog C≡O, which can be protonated at O and forms a symmetric $O\cdots H^+\cdots O$ proton-bound dimer. The sp^2-hybridized S bases often form complexes with symmetric hydrogen bonds as do their first-row counterparts. These dimers include $(S{=}C{=}S)_2H^+$, $(H_2C{=}S)_2H^+$, $(MeHC{=}S)_2H^+$, $(Me_2C{=}S)_2H^+$, and $(FHC{=}S)_2H^+$. However, electron-withdrawing F substituents lead to an asymmetric proton-bound dimer for $(F_2C{=}S)_2H^+$, whereas $(F_2C{=}O)_2H^+$ is symmetric. This difference between first-row and second-row $(F_2C{=}X)_2H^+$ dimers may be associated with the lower electronegativity of S, as well as its greater polarizability, both of which make it more sensitive to substituent effects.

The proton-bound dimer of H_2S has an asymmetric hydrogen bond, although the energies of the symmetric and

asymmetric structures are essentially identical over a range of distances, as demonstrated by the distortion energy curve shown in Sect. 3.4. However, methyl substitution increases the basicity of S and allows MeHS and Me_2S to form symmetric proton-bound dimers. Like the sp^2 base $F_2C{=}S$, proton-bound dimers of the sp^3 bases FHS and F_2S have asymmetric bonds. Such is not the case for corresponding proton-bound sp^3 dimers of O bases, all of which have symmetric hydrogen bonds. However, the symmetrization energies of asymmetric dimers of S bases are quite small at 2–3 kJ mol^{-1}.

The *sp*-hybridized bases HC≡P and MeC≡P do not protonate at P nor do they form stable proton-bound dimers at P [30]. This is similar to the *sp*-hybridized S base C≡S, but notably different from the corresponding *sp*-hybridized N bases, which usually form symmetric N···H^+···N proton-bound dimers. The sp^2 and sp^3 proton-bound dimers of P bases are asymmetric, as are the corresponding N dimers. The P dimers have much greater symmetrization energies, reflecting both the lower electronegativity of P and the longer P···P distances.

There are other secondary factors that also influence the detailed structures of proton-bound homodimers of the first-row and second-row bases. For example, bond angles are generally considerably narrower at second-row atoms than at first-row atoms. The structures of the protonated ions and the proton-bound dimers of corresponding sp^2-hybridized bases $H_2C{=}O$ and $H_2C{=}S$ demonstrate the difference. Fig. 3 displays the equilibrium structures of $H_2C{=}OH^+$ and the proton-bound dimer $(H_2C{=}O)_2H^+$. The C–O–H angle is 114° in $H_2C{=}OH^+$ and 119° in $(H_2C{=}O)_2H^+$. In contrast, the C–S–H angle is 98° in $H_2C{=}SH^+$ and 93° in the dimer $(H_2C{=}S)_2H^+$. Thus, the angle at which a base is protonated is reflected in the structure of the corresponding proton-bound dimer.

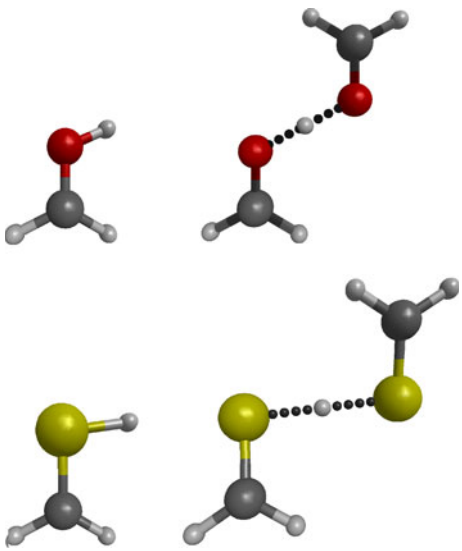

Fig. 3 The structures of $H_2C{=}OH^+$, $(H_2C{=}O)_2H^+$, $H_2C{=}SH^+$, and $(H_2C{=}S)_2H^+$

The pairs of C–N–H and C–P–H bond angles in the protonated sp^2-hybridized bases $H_2C{=}NH_2^+$ and $H_2C{=}PH_2^+$ are equivalent and have values of 121° for both systems. The similarities in the bond angles at N and P are also seen in the corresponding proton-bound dimers, which have C_1 symmetry. For $(H_2C{=}NH)_2H^+$, the C–N–H angle for the proton-donor molecule is 121°, while the H–N–C angle for the proton acceptor is 129°. The corresponding angles for $(H_2C{=}PH)_2H^+$ are 121° and 126°, respectively. Of course, the neutral molecules $H_2C{=}NH$ and $H_2C{=}PH$ have only one H atom bonded to N or P, so the difference between corresponding first-row and second-row bases appears once again as the H–X–C angles are 110° and 97°, respectively.

Another factor that influences the structure and stability of a proton-bound dimer is the existence of long-range interactions, that is, interactions involving atoms or groups of atoms in addition to those directly involved in the X···H^+···X hydrogen bond. These interactions may be either attractive or repulsive and are evident in proton-bound dimers when (non-H-bonding) H atoms of the parent bases are replaced by substituents such as F or CH_3. The effects of such long-range interactions can readily be seen by comparing the BEs and structures of the isomers of $(FHC{=}S)_2H^+$ and $(MeHC{=}S)_2H^+$ with symmetric hydrogen bonds, in which the substituents are cis and trans to the hydrogen-bonding region with respect to the C=S bond. For this comparison, the structure of the cis isomer of $(FHC{=}S)_2H^+$ was optimized under the constraint of C_{2h} symmetry since that is the symmetry of the cis isomer of $(MeHC{=}S)_2H^+$. Fig. 4 displays these dimers, and Table 2 provides relative BEs, S···S distances, and C–S···H angles.

The BEs of both isomers of $(MeHC{=}S)_2H^+$ are greater than the BEs of the isomers of $(FHC{=}S)_2H^+$, as expected (see Fig. 2 and Table 2). However, the more stable isomer of $(MeHC{=}S)_2H^+$ has the methyl group trans to the hydrogen-bonding region, while the more stable $(FHCS)_2H^+$ isomer has the F atom cis to the hydrogen-bonding region (Table 2). Having the methyl groups "trans" to the hydrogen bond reduces repulsive interactions. On the other hand, the "cis" structure of $(FHC{=}S)_2H^+$ provides a favorable interaction between the F atoms and the hydrogen-bonded proton, which in turn compensates for other repulsive interactions. The repulsive interactions in the cis isomer of $(MeHC{=}S)_2H^+$ are also reflected in its structure. Thus, it has the longest S···S distance as well as the widest C–S···H angle. Long-range interactions are also responsible for making the equilibrium structure of the asymmetric phosphinine dimer $(C_5H_5P)_2H^+$ C_{2v} perpendicular rather than planar, in agreement with the equilibrium structure of its first-row counterpart pyridine dimer $(C_5H_5N)_2H^+$.

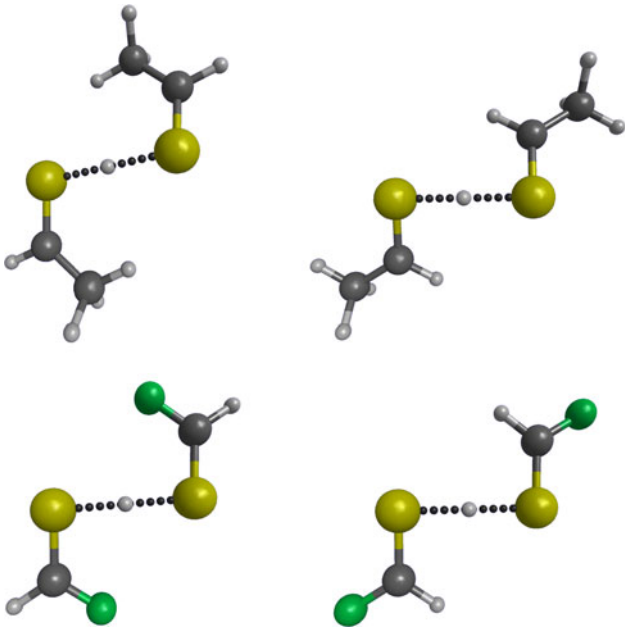

Fig. 4 The cis and trans C_{2h} isomers of $(MeHC{=}S)_2H^+$ and $(FHC{=}S)_2H^+$

Table 2 MP2/6-311+G(2df,p) relative energies [ΔE, kJ mol^{-1}], S···S distances (Å) and C–S···H angles (°) of the cis and trans isomers of $(MeHC{=}S)_2H^+$ and $(FHC{=}S)_2H^+$ with C_{2h} symmetry

Dimer	Isomer	ΔE	R(S···S)	∠C–S···H
$(MeHC{=}S)_2H^+$	Cis	13.7	3.326	101
	Trans	0.0	3.287	93
$(FHC{=}S)_2H^+$	Cis	0.0	3.321	95
	Trans	11.6	3.309	91

3.4 Symmetrization energies and distortion energies of second-row proton-bound dimers

To further examine the factors that govern the structures of proton-bound dimers, we examined their symmetrization energies (ΔE_{sym}) and distortion energies (ΔE_{dist}). Figure 5 provides a plot of ΔE_{sym} values for second-row proton-bound dimers versus the PAs of the second-row bases. As observed previously for proton-bound first-row dimers [22], this diagram clearly illustrates that ΔE_{sym} of second-row proton-bound dimers are not determined by PAs. It also shows that the ΔE_{sym} of homodimers with Cl bases are zero (i.e., the structures are symmetrical), those with S bases are less than a few kJ mol^{-1}, whereas those for P bases vary from about 15 to 40 kJ mol^{-1} and are therefore much greater than ΔE_{sym} of first-row N homodimers [22]. This reflects in part the low electronegativity of P bases and the much longer P···P equilibrium distances in these proton-bound dimers, which must contract significantly to form a symmetric hydrogen bond.

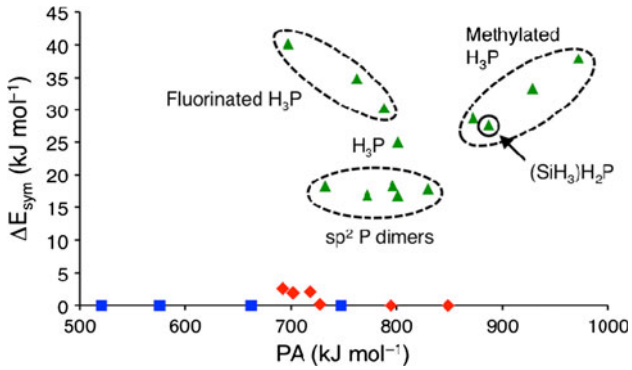

Fig. 5 Symmetrization energies (ΔE_{sym}, kJ mol^{-1}) versus proton affinities (PA, kJ mol^{-1}) of proton-bound homodimers of bases containing Cl (*filled square*), S (*filled diamond*), and P (*filled triangle*)

There is an interesting arrangement of points in Fig. 5 belonging to dimers with P–H$^+$···P hydrogen bonds, and these points can be grouped according to the hybridization of P and the nature of the substituents. There are five points that have ΔE_{sym} values between 15 and 20 kJ mol^{-1} that belong to the proton-bound sp^2-hybridized dimers of $H_2C{=}PH$, $MeHC{=}PH$, $Me_2C{=}PH$, $(SiH_3)HC{=}PH$, and C_5H_5P. There are eight points for dimers in which P is sp^3 hybridized that have higher ΔE_{sym} values, and these form what might be described as a "V" in this plot. The point at the bottom of the "V" belongs to $(H_3P)_2H^+$. Those to the left and higher in symmetrization energy correspond to the three fluoro-substituted H_3P dimers; points to the right and higher in symmetrization energy than H_3P are the three proton-bound methyl-substituted H_3P dimers and the proton-bound dimer of $(SiH_3)H_2P$.

For both the methyl- and fluoro-substituted bases, the proton-bound dimers of the trisubstituted derivatives have the highest symmetrization energies, while the monosubstituted dimers have the lowest. What could account for the increase in symmetrization energies with increasing number of substituents in both the fluoro- and methyl-substituted proton-bound dimers? Upon examination of the structures of the dimers, we find a correlation between ΔE_{sym} and the P···P distances (Fig. 6). Thus, as the P···P distance increases, a greater contraction of this distance is required to form a symmetric hydrogen bond, resulting in a larger ΔE_{sym}. The P···P distance increases with the number of substituents, which may reflect increased repulsive interactions between the substituents, especially in the symmetric structures. It is also evident from this figure that the effect of the substituent on the P···P distance, and hence ΔE_{sym}, is greater for F than for Me groups.

How do the distortion energies for proton-bound dimers vary? Figure 7 presents plots of ΔE_{dist} versus Δr for the first-row proton-bound dimers $(HF)_2H^+$, $(H_2O)_2H^+$, and $(H_3N)_2H^+$ and the corresponding second-row proton-bound

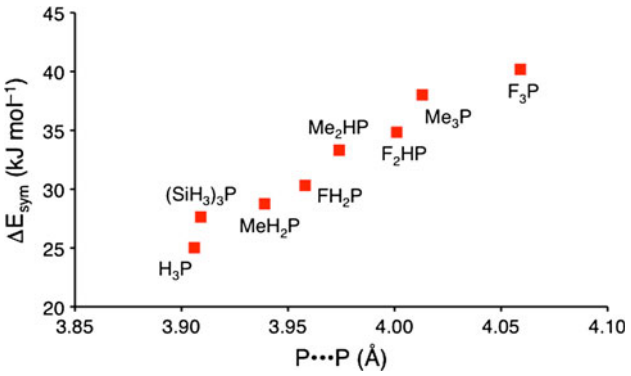

Fig. 6 Symmetrization energies (ΔE_{sym}, kJ mol^{-1}) versus the P···P distance (Å) in H_3P and substituted H_3P proton-bound dimers

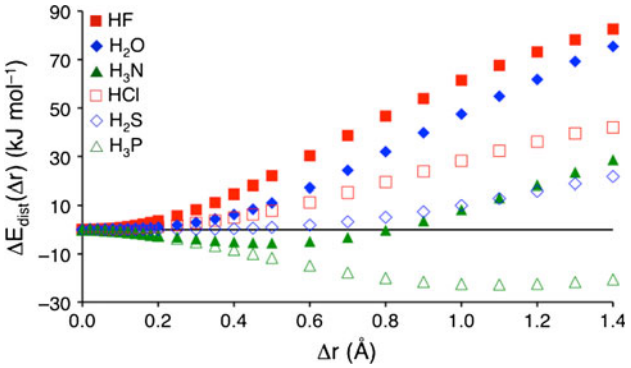

Fig. 7 MP2/6-311+G(2df,p) distortion energies ($\Delta E_{dist}(\Delta r)$, kJ mol^{-1}) of proton-bound first-row and second-row homodimers as a function of the difference between the X–H bond lengths across X–H$^+$···X hydrogen bonds (Δr, Å)

dimers $(HCl)_2H^+$, $(H_2S)_2H^+$, and $(H_3P)_2H^+$. We loosely classify the distortion energy curves in Fig. 7 into three types. Those for $(HF)_2H^+$, $(H_2O)_2H^+$, and $(HCl)_2H^+$ increase as Δr increases since the equilibrium structures of these dimers are symmetric. Curves for $(H_3N)_2H^+$ and $(H_3P)_2H^+$ decrease initially until Δr becomes equal to the difference between the two X–H distances in the equilibrium structure and then increase. The curve for $(H_2S)_2H^+$ is in between, with a very flat potential in the region near the minimum. At the highest level of theory used to investigate the $(H_2S)_2H^+$ complex [CCSD(T)/6-311+G(2df,p)], it retains an asymmetric structure, but with a symmetrization energy of just 1.8 kJ mol^{-1}.

The potential curves for these dimers indicate that distorting the hydrogen bond away from its symmetric structure is much easier for the second-row dimer $(HCl)_2H^+$ than for $(HF)_2H^+$ and $(H_2O)_2H^+$. At each value of Δr in the range from 0.0 to 1.4 Å, the order of curves from greatest to least distortion energy is $(HF)_2H^+ > (H_2O)_2H^+ > (HCl)_2H^+$. In general, the X···H$^+$···X potential curves show that distortions from symmetric structures are easier for second-row dimers than for their first-row counterparts, which may also be a consequence of their significantly longer intermolecular X···X equilibrium distances, as evident from Table 3.

Table 3 X···X and X–H distances (R, Å) and binding energies (BE, kJ mol^{-1}) for proton-bound dimers of first-row and second-row hydrides

Dimers	Symmetric HB		Asymmetric HB		BE[a]
	R(X···X)	R(X–H)	R(X···X)	R(X–H)	
$(HF)_2H^+$	2.288	1.144			137
$(H_2O)_2H^+$	2.384	1.192			142
$(H_3N)_2H^+$	2.602	1.301	2.686	1.129	109
$(HCl)_2H^+$	3.132	1.566			78
$(H_2S)_2H^+$	3.328	1.664	3.333	1.615	61
$(H_3P)_2H^+$	3.490	1.745	3.906	1.421	32

[a] MP2/6-311+G(2df,p) binding energies

A closer examination of Fig. 7 indicates that there is a crossing of the curves for $(H_2S)_2H^+$ and $(H_3N)_2H^+$ at Δr ~ 1.1 Å. Two other curve crossings arise as Δr increases further, one involving $(H_2O)_2H^+$ and $(HF)_2H^+$, and the other involving $(H_3N)_2H^+$ and $(HCl)_2H^+$. These occur because the potential curves asymptotically approach a limit corresponding to the energy of dissociation to the appropriate isolated neutral and protonated bases. This limit is equal to the binding energy in the case of symmetric complexes, and the binding energy minus ΔE_{sym} (Eq. 3) in the case of asymmetric structures. At the MP2/6-311+G(2df,p) level, the asymptotic ordering is $(H_3P)_2H^+$ (12 kJ mol^{-1}) < $(H_2S)_2H^+$ (61 kJ mol^{-1}) < $(HCl)_2H^+$ (78 kJ mol^{-1}) < $(H_3N)_2H^+$ (107 kJ mol^{-1}) < $(HF)_2H^+$ (137 kJ mol^{-1}) < $(H_2O)_2H^+$ (142 kJ mol^{-1}).

4 Conclusions

High-level ab initio quantum chemical calculations have been used to examine proton-bound homodimers of second-row bases and compare them with their first-row analogs. The following important points emerge from the present study.

1. The relationship between the binding energies (BEs) of second-row dimers and the proton affinities (PAs) of the corresponding bases follows the same pattern as that for the first-row systems, with the binding energies initially increasing with increasing proton affinity but subsequently decreasing. This non-monotonic trend may be attributed to the opposing effects of increased PA on the hydrogen-bond (HB) donor and HB acceptor.
2. The PAs of the first-row and second-row bases are influenced by the charge on the proton-acceptor atom

and its polarizability. These two effects oppose one another, with the polarizability usually dominant and leading to higher PAs for Ar, HCl, and H_2S compared with their first-row counterparts. However, the positive charge on P leads to a lower PA for H_3P than for H_3N. Second-row dimers generally have smaller BEs than those for the corresponding first-row dimers. This can usually be attributed to the smaller negative charge at the HB acceptor atom.

3. There is a reduced tendency for second-row homodimers to form symmetrical hydrogen bonds compared with the corresponding first-row dimers. This may be attributed to the longer internuclear separations between second-row atoms, as well as to their lower electronegativities relative to their first-row analogs. Finer structural details of the dimers are related to the structures of the corresponding protonated monomers and are also influenced by long-range attractive and repulsive interactions.

Acknowledgments We gratefully acknowledge the award of an Australian Professorial Fellowship and funding from the ARC Centre of Excellence for Free Radical Chemistry and Biotechnology (to L.R.), and generous allocations of computer time from the National Computational Infrastructure (NCI) National Facility and Intersect Australia Ltd, and from the Ohio Supercomputer Center.

References

1. Jeffrey GA (1997) An introduction to hydrogen bonding. Oxford University Press, New York
2. Scheiner S (ed) (1997) Hydrogen bonding: a theoretical perspective. Oxford University Press, New York
3. Scheiner S (1997) Molecular interactions: from van der Waals to strongly bound complexes. John Wiley and Sons, Chichester
4. Grabowski SJ (ed) (2006) Hydrogen bonding—new insights. Springer, Dordrecht
5. Buckingham AD, Del Bene JE, McDowell SAC (2008) Chem Phys Lett 463:1–10
6. Gilli G, Gilli P (2009) The nature of the hydrogen bond: outline of a comprehensive hydrogen bond theory. Oxford University Press, Oxford
7. Zeegers-Huyskens T (1988) J Mol Struct 177:125–141
8. Gilli G, Gilli P (2000) J Mol Struct 552:1–15
9. Humbel S, Hoffmann N, Cote I, Bouquant J (2000) Chem Eur J 6:1592–1600
10. Humbel S (2002) J Phys Chem A 106:5517–5520
11. Bian L (2003) J Phys Chem A 107:11517–11524
12. Mautner M (2005) Chem Rev 105:213–284
13. Del Bene JE, Elguero J, Alkorta I (2007) J Phys Chem A 111:3416–3422
14. Hibbert F, Emsley J (1990) Adv Phys Org Chem 26:255–379
15. Schiøtt B, Iversen BB, Madsen GKH, Bruice TC (1998) Proc Natl Acad Sci USA 95:12799–12802
16. Overgaard J, Schiøtt B, Larsen FK, Schultz AJ, John C, MacDonald JC, Iversen BB (1999) Angew Chem Int Ed 38:1239–1242
17. Gilli P, Bertolasi V, Ferretti V, Gilli G (2000) J Am Chem Soc 122:10405–10417
18. Pauling LC (1960) The nature of the chemical bond. Cornell University Press, New York
19. Desiraju G, Steiner T (1999) The weak hydrogen bond in structural chemistry and biology. Oxford University Press, New York
20. Marechal Y (2007) The hydrogen bond and the water molecule: the physics and chemistry of water, aqueous and biomedia. Elsevier, Amsterdam
21. Chan B, Del Bene JE, Radom L (2007) J Am Chem Soc 129:12197–12199
22. Chan B, Del Bene JE, Radom L (2009) Mol Phys 107:1095–1105
23. Hehre WJ, Radom L, Schleyer PvR, Pople JA (1986) Ab initio molecular orbital theory. Wiley, New York
24. Jensen F (2006) Introduction to computational chemistry, 2nd edn. Wiley, Chichester
25. Frisch MJ, Trucks GW, Schlegel HB, Scuseria GE, Robb MA, Cheeseman JR, Montgomery Jr JA, Vreven T, Kudin KN, Burant JC, Millam JM, Iyengar SS, Tomasi J, Barone V, Mennucci B, Cossi M, Scalmani G, Rega N, Petersson GA, Nakatsuji H, Hada M, Ehara M, Toyota K, Fukuda R, Hasegawa J, Ishida M, Nakajima T, Honda Y, Kitao O, Nakai H, Klene M, Li X, Knox JE, Hratchian HP, Cross JB, Bakken V, Adamo C, Jaramillo J, Gomperts R, Stratmann RE, Yazyev O, Austin AJ, Cammi R, Pomelli C, Ochterski JW, Ayala PY, Morokuma K, Voth GA, Salvador P, Dannenberg JJ, Zakrzewski VG, Dapprich S, Daniels AD, Strain MC, Farkas O, Malick DK, Rabuck AD, Raghavachari K, Foresman JB, Ortiz JV, Cui Q, Baboul AG, Clifford S, Cioslowski J, Stefanov BB, Liu G, Liashenko A, Piskorz P, Komaromi I, Martin RL, Fox DJ, Keith T, Al-Laham MA, Peng CY, Nanayakkara A, Challacombe M, Gill PMW, Johnson B, Chen W, Wong MW, Gonzalez C, Pople JA (2004) Gaussian 03, revision E01. Gaussian, Inc., Wallingford CT
26. Frisch MJ, Trucks GW, Schlegel HB, Scuseria GE, Robb MA, Cheeseman JR, Scalmani G, Barone V, Mennucci B, Petersson GA, Nakatsuji H, Caricato M, Li X, Hratchian HP, Izmaylov AF, Bloino J, Zheng G, Sonnenberg JL, Hada M, Ehara M, Toyota K, Fukuda R, Hasegawa J, Ishida M, Nakajima T, Honda Y, Kitao O, Nakai H, Vreven T, Montgomery Jr JA, Peralta JE, Ogliaro F, Bearpark M, Heyd JJ, Brothers E, Kudin KN, Staroverov VN, Kobayashi R, Normand J, Raghavachari K, Rendell A, Burant JC, Iyengar SS, Tomasi J, Cossi M, Rega Millam NJ, Klene M, Knox JE, Cross JB, Bakken V, Adamo C, Jaramillo J, Gomperts RE, Stratmann O, Yazyev AJ, Austin R, Cammi C, Pomelli JW, Ochterski R, Martin RL, Morokuma K, Zakrzewski VG, Voth GA, Salvador P, Dannenberg JJ, Dapprich S, Daniels AD, Farkas O, Foresman JB, Ortiz JV, Cioslowski J, Fox DJ (2009) Gaussian 09, revision A02. Gaussian, Inc., Wallingford CT
27. Swart M, Rösler E, Bickelhaupt FM (2006) J Comput Chem 27:1486–1493
28. Schwerdtfeger P (2010) The CTCP table of experimental and calculated static dipole polarizabilities for the electronic ground states of the neutral elements. Massey University, Auckland. URL: http://ctcp.massey.ac.nz/dipole-polarizabilities
29. Chan B, Del Bene JE, Elguero J, Radom L (2005) J Phys Chem A 109:5509–5517
30. Alkorta I, Elguero J, Del Bene JE (2007) J Phys Chem A 111:9924–9930